Curr Cell Biochem 2011 1(1): 1-14

Current Cellular Biochemistry

www.academyjournals.net

Original Article

Differential nuclear staining assay for high-throughput screening to identify cytotoxic compounds

Carolina LEMA, Armando VARELA-RAMIREZ*, Renato J. AGUILERA

University of Texas at El Paso, Department of Biological Sciences, Bioscience Research Building, 500 West University Ave. El Paso, Texas 79968-0519, USA

Received: 25.07.2011 ***Accepted: 04.09.2011*** ***Published: 12.09.2011***

Abstract

As large quantities of novel synthetic molecules continue to be generated there is a challenge to identify therapeutic agents with cytotoxic activity. Here we introduce a Differential Nuclear Staining (DNS) assay adapted to live-cell imaging for high throughput screening (HTS) that utilizes two fluorescent DNA intercalators, Hoechst 33342 and Propidium iodide (PI). Since Hoechst can readily cross cell membranes to stain DNA of living and dead cells, it was used to label the total number of cells. In contrast, PI only enters cells with compromised plasma membranes, thus selectively labeling dead cells. The DNS assay was successfully validated by utilizing well known cytotoxic agents with fast or slow cytotoxic activities. The assay was found to be suitable for HTS with Z' factors ranging from 0.86 to 0.60 for 96 and 384-well formats, respectively. Furthermore, besides plate-to-plate reproducibility, assay quality performance was evaluated by determining ratios of signal-to-noise and signal-to-background, as well as coefficient of variation, which resulted in adequate values and validated the assay for HTS initiatives. As proof of concept, eighty structurally diverse compounds from a small molecule library were screened in a 96-well plate format using the DNS assay. Using this DNS assay, six hits with cytotoxic properties were identified and all of them were also successfully identified by using the commercially available MTS assay (CellTiter 96® Cell Proliferation Assay). In addition, the DNS and a flow cytometry assay were used to validate the activity of the cytotoxic compounds. The DNS assay was also used to generate dose-response curves and to obtain CC_{50} values. The results indicate that the DNS assay is reliable and robust and suitable for primary and secondary screens of compounds with potential cytotoxic activity.

***Key words**: Drug discovery; High-content screening; Hit identification; Image-based assay; Live-cell fluorescence assay; Propidium iodide.*

**Co-first author and corresponding author. A. Varela-Ramirez, e-mail: avarela2@utep.edu Phone 1- 915 747-8812, Fax 1- 915 747-5808*

INTRODUCTION

Live-cell imaging applications have been gaining substantial attention due to the emergence of novel automated microscopic technology and the creation of highly sophisticated software for image acquisition and quantitative analysis. Capturing automated images in real time and its associated quantitative analysis is very reliable, fast and robust (Pepperkok and Ellenberg 2006). The capacity to monitor how cells respond when exposed to a new chemical compound is a crucial aspect in drug discovery, cell biology and many other biomedical areas. Furthermore, an essential component in anticancer-drug discovery involves determining the cytotoxic activity of test compounds in a quantitative and reliable manner (Gonzalez-Nicolini and Fussenegger 2005).

The measure of membrane integrity is one of the most direct and reliable methods to assess cellular viability (Kroemer et al. 2005). Vital dyes such as Trypan blue and Propidium iodide (PI) only enter cells after the cell membrane has been compromised (Parks et al. 1979; Yuhas et al. 1974). Although the Trypan blue viability assay utilizes simple equipment and is inexpensive, it is very time consuming. On the other hand, the use of PI requires specialized instrumentation capable to exciting this fluorophore and detecting its emitted fluorescence.

Methods for determining cell membrane integrity have also been established by quantifying the leakage of components from the cytoplasm into the surrounding culture

medium, in which the number of lysed cells is proportional to the "released" enzymatic activity. An example of this type of analysis is the lactate dehydrogenase (LDH) assay, where the activity of LDH released by dead cells is measured in the supernatant of culture wells (Decker and Lohmann-Matthes 1988). An improved fluorescent variant of this technique detects the LDH released from dead cells in the presence of living cells. This is measured selectively without damaging membranes of the viable cell population, by using a coupled enzymatic method that converts resazurin into the fluorescent compound, resorufin (Riss and Moravec 2002). However, a disadvantage of the LDH release assay is that it is not applicable to compounds that interfere with LDH activity (Sasaki and Ohno 1994). In addition, the LDH activity present in most serum-containing growth media affects the readout by increasing the background and thus limits the sensitivity of the assay. While background LDH activity can be avoided by minimizing the amount of serum in the media, this may result in decreased cell viability at longer time points (Batchelor and Zhou 2004).

Colorimetric assays have also been developed that measure metabolic activity by reducing MTT (3-(4,5-dimethylthiazol-2-yl)-2,5-diphenyltetrazolium bromide) or MTS (3-(4,5-dimethylthiazol-2-yl)-5-(3-carboxymethoxyphenyl)-2-(4-sulfophenyl)-2H-tetrazolium) reagents to formazan dyes, mainly via mitochondrial succinate dehydrogenase resulting in a substrate color change (from yellow to purple). Although relatively inexpensive and fast, these assays cannot provide a direct measure of cell death as other factors may influence cellular enzymatic activity (discussed in detail by Kepp et al. 2011). In addition, some phenolic compounds can reduce the MTT to formazan in the absence of cells (Bruggisser et al. 2002). It has also been recently reported that MTT/MTS-based assays can underestimate the antiproliferative activity of green tea polyphenols in prostate and breast cancer cells (Wang et al. 2010).

The jellyfish-derived green fluorescent protein (GFP) and its spectral variants possess an ample variety of biological applications, including methods to study cytotoxicity (Miyawaki et al. 2005; Verkhusha and Lukyanov 2004; Zhang et al. 2002). In previous work, we have developed a simple fluorescence-based assay for the rapid screening of potential cytotoxic compounds that consisted on using GFP-expressing HeLa cells (Montoya et al. 2004; Aguilera et al. 2006). Addition of a cytotoxic compound to the GFP-labeled cells resulted in the reduction of GFP fluorescence intensity that was readily measured by fluorometry and microscopy (Montoya et al. 2004: Montoya et al. 2005). Moreover, the assay's flexibility allowed its application for tandem screening of anticancer and antibacterial compounds (Montoya et al. 2005). Apart from the difficulty in establishing stable GFP-expressing lines, it has been reported that GFP-expressing cells are more sensitive to a variety of anticancer drugs apparently due to an increase in cellular oxidative stress (Goto et al. 2003). Therefore, while GFP expression is highly useful for a large number of applications, it may not be as useful for cytotoxicity or other cellular assays (Goto et al. 2003).

Progression of both necrosis and apoptosis will eventually culminate with cell death, which is manifested by plasma membrane disruption, allowing impermeable dyes like PI to selectively label the nuclei of dead cells. Recently, the very well established method to distinguish apoptosis and necrosis, utilizing Annexin V and PI, has been adapted to live-cell imaging to monitor nerve cell death in the eyes of live rats (Cordeiro et al. 2010). Time-lapse imaging has been implemented to examine apoptosis or cell viability, without subsequent manipulation of the cellular surroundings in cell cultures, using Annexin-based probes (Dragunow 2008; Kim et al. 2009). On the other hand, high-content screening cell-based assays have been used extensively in modern drug discovery and other fields using automated approaches. For instance, high-content imaging has been applied on the study of regulation of neuronal signaling pathways (Chan et al. 2005), androgen receptor function (Szafran et al. 2008), assessment of parasite-host cell infection rates (Nohara et al. 2010), discovery of antileishmanial (Siqueira-Neto et al. 2010) and antitrypanosomal compounds (Engel et al. 2010; Romanha et al. 2010), and evaluation of anticancer compound activities (Gonzalez-Nicolini and Fussenegger 2005; Tian et al. 2007). In addition, there are large numbers of articles that describe HTS assays for mitosis regulators as potential targets for cancer therapy, detection of small molecule inhibitors of signaling, trafficking, and other biochemical pathways (Ahmed et al. 2010; Bartholomeusz et al. 2007; Chan et al 2005; Rosado et al. 2008; Zanella et al. 2008).

Combined staining with Hoechst and PI has been previously applied to analyze dead and living cell distributions by flow cytometry (Ciancio et al. 1988; Dive et al. 1992; Lau et al. 2007; Stohr and Vogt-Schaden 1980; Wallen et al. 1983). This double staining approach combined with automated cellular imaging has been previously applied to adherent neural cell cultures in a 96-well plate format to determine cell viability but this assay was not validated for HTS (Breier et al. 2008). In the present report, we describe the adaptation and validation for HTS of the differential nuclear (DNS) staining strategy to measure compound cytotoxicity in adherent and non-adherent cells in 96- and 384-well plate formats *via* HTS automated microscopy.

Microscope images of adherent cells are relatively easy to capture since they are localized at the bottom of the well and most of the cells are in the same focal plane of the objective lens. In contrast, capturing images of non-adherent cells is

more challenging, because they have a tendency to form aggregates, creating a variety of focal planes that may result in out of focus images. In this context, it was hypothesized that due to the stationary nature of the bioimager stage, and its movable optics, the assay proposed here could be utilized for both adherent and non-adherent cells. To verify the effectiveness of the DNS assay, two cell lines from different species, tissue origin, dissimilar morphology and growth properties: an adherent fibroblastic (NIH 3T3) and a non-adherent lymphoid YT NK-like (YT) cell lines were utilized for comparison purposes. The BD Pathway 855 bioimager was utilized to automatically detect the fluorescent signals of both dyes, and cell death was subsequently determined by calculating the percentage of dead cells (PI positive) in each well. In the present study, the DNS assay was evaluated for its utility as an HTS assay by determining the Z' factor value, signal-to-background (S/B) and signal-to-noise (S/N) ratios (Zhang et al. 1999), as well as the coefficient of variation (%CV; Inglese et al. 2007). Moreover, the DNS assay was utilized for hit identification, hit validation, generation of dose-response curves and CC_{50} values. The DNS assay allows data generation at the single-cell level, without subjecting the cells to any manipulation other than addition of the dye mixture prior to image acquisition; thus greatly reducing the processing time. Moreover, the live-cell DNS assay provides a highly precise measurement of live and dead cells that can be visually verified after image capture. A workflow of the DNS assay adapted to 96 and 384-well plates is shown in Figure 1.

MATERIAL AND METHODS

Experimental compounds and reagents

As proof of principle, eighty experimental chemical compounds were used in the present study which were included in a single plate (Plate 60216) that was randomly chosen from the DIVERSet small molecule library (Code NT797; ChemBridge Corporation, San Diego, CA). The ChemBridge ID number, chemical structure, molecular weight and molecular name of the experimental chemical compounds are available upon request. Compound stock solutions were received already dissolved in Dimethyl sulfoxide (DMSO) and dilutions of each of them were added directly to individual wells containing target cells in complete culture media. Hoechst 33342 (Hoechst; Invitrogen, Eugene, OR); and Propidium iodide (PI; MP Biomedicals, Solon, OH) stock solutions were mixed, diluted in cell culture media and added to each experimental well at a final concentration of 1 µg/ml for each dye.

Cell lines and culture conditions

Two cell lines were utilized in the implementation of this DNS assay, the adherent NIH 3T3 murine fibroblast cells (American Type Culture Collection, Manassas, VA; CRL-1658), and the non-adherent YT human lymphoma cells (Yodoi et al. 1985). The culture media for adherent cells was DMEM (HyClone, Logan, UT) plus 10% heat-inactivated newborn calf serum (HyClone), while that for non-adherent cells was RPMI (HyClone) media containing 10% heat inactivated fetal bovine serum (HyClone). Both culture media were supplemented with 100 U/ml penicillin, 100 µg/ml streptomycin, and 0.25 µg/ml amphotericin B (Lonza, Walkersville, MD). The incubation conditions of the cells were at 37ºC in humidified 5% carbon dioxide (CO_2) atmosphere, in a regular water jacketed incubator or the environmentally controlled chamber of the bioimaging system. To prepare the experimental multiwell plates and to guarantee high viability, adherent cells were washed with fresh media to eliminate cell debris and floating cells consisting mainly of dead cells. When necessary, the viability of non-adherent cells was increased by using Ficoll-Paque™PLUS density gradient centrifugation (Boyum 1968). Briefly, after centrifugation at 400xg for 30 min at room temperature, live cells at the interface were collected and washed with fresh culture media. Subsequently, these non-adherent cells were expanded by starting a new culture. Only cultures containing cell viabilities of 95% or higher were used for the cytotoxicity studies. NIH 3T3 were harvested from culture flasks by adding 2 ml of 0.25% trypsin solution (Invitrogen, Carlsbad, CA), diluted in serum free DMEM, and incubated for approximately 5 min at 37°C. Trypsin was neutralized by addition of culture media with 10% serum. NIH 3T3 and YT cells were seeded at a cell density of 15,000 and 10,000 cells/well, respectively, in glass-bottomed 96-well plates (BD Biosciences, Rockville, MD) using 200 µl of culture media/well. When the 384-well plate format (BD Biosciences) was utilized, NIH 3T3 and YT cells were seeded at a density of 3,750 and 2,500 cells per well in a volume of 50 µl culture media, respectively. For the MTS assay, NIH 3T3 cells were seeded at 15,000 cells in 100 µl of media culture per well in a flat-bottomed plastic 96-well plate (Falcon, Franklin Lakes, NJ). Cell seeding was achieved with a robotic pipette system (epMotion 5070, Eppendorf, New York, NY). Multiwell plates containing cells were incubated overnight in culture media prior to addition of the chemical compounds.

Image acquisition and analysis

The BD Pathway 855 bioimager system and its associated AttoVision v1.6.2 software (BD Biosciences, Rockville, MD) were utilized for image collection and analysis. After dye addition and incubation, images were captured with two

software predetermined excitation/emission filter sets; 380/535 nm for Hoechst and 555/645 nm for PI. Images from each well were acquired using a 20x/ NA 0.75 dry objective. In order to obtain sufficient cell numbers (ROIs) for statistically robust data, images from four contiguous fields (2x2 montage) were obtained per well. Under these settings and by plating NIH 3T3 and YT cells at the cell densities indicated above, the system was able to capture from ~100 to 400 cells per well and the images were subsequently analyzed using the AttoVision software. To define nuclei as individual units or regions of interest (ROIs), pre-processing filters and intensity thresholds were applied for image segmentation. Segmented images were subjected to data classification by the use of the AttoVision software. The percentage of dead cells was calculated from the total number of ROIs per well. Cell nuclei emitting fluorescence signal from both Hoechst and PI (fluorescence co-localization) were considered as dead cells, while cells emitting only Hoechst signal were counted as live cells. Data was classified by the use of the AttoVision software to identify compounds with cytotoxic activity and hits were identified by applying the 2xSD principle (see below).

Validation of the DNS assay with known toxic and non-toxic compounds

Validation of the DNS assay was performed utilizing NIH 3T3 cells, 96-well plates, and a panel of 10 compounds with known toxic or non-toxic activity.

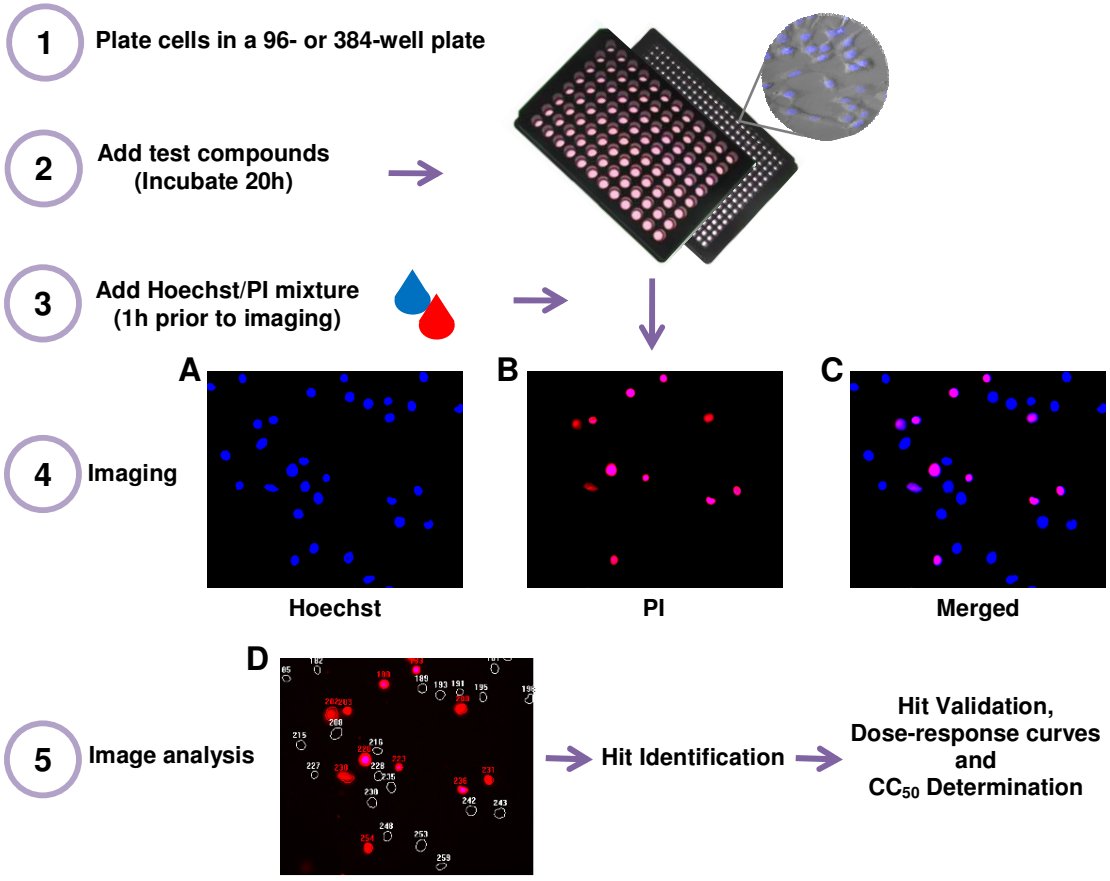

Figure 1. Workflow of the DNS assay. The assay consists of five stages: (1) cell seeding, (2) compound addition, (3) dyes addition, (4) image acquisition, and (5) image/data analysis. Representative fluorescence images correspond to NIH 3T3 cells after exposure for 20h to a cytotoxic compound. Since the bioimager system is equipped with a monochrome camera, it was necessary to apply computerized pseudo color to each fluorescence channel to achieve the colored images. The four microscopic images in panels A, B, C and D, correspond to the same image field of a 2x2 montage, captured with a 20x objective utilizing the bioimager and the AttoVision software. In panel A, Hoechst stained live and dead cell nuclei are shown in blue and comprise the total number of cells. Whereas in panel B, Propidium iodide (PI) stained dead cells nuclei are denoted in red. In panel C, merged Hoechst and PI images result in magenta colored nuclei due to co-localization of both fluorescence signals in dead cells. In panel D, segmented images are shown, where nuclei of live cells are delimited by a white line and nuclei of dead cells appear as solid red dots.

Three antibiotics: ampicillin (Fisher Scientific, Pittsburgh, PA), kanamycin (Fisher Scientific) and streptomycin (Fisher Scientific) were included as non-toxic compounds at a final concentration of 100 µg/ml. Also, seven compounds that cause toxic effects on mammalian cells were utilized at final concentrations indicated as follows: 100 µM Cisplatin (Strem Chemicals, Newburyport, MA), 1444 µM Geneticin (G418; Sigma-Aldrich, Inc., St Louis, MO), 379 µM hygromycin B (EMD Chemicals, Gibbstown, NJ), 10 µM iodoacetamide (Sigma), 20 µM plumbagin (Sigma), 500 µM titanocene (Sigma), and 0.1% v/v Tween 20 (Acros Organics, New Jersey). An initial experiment included all ten compounds incubated for 20h, to detect those with fast activity. A second experiment extended the incubation time for 72h and 120h in order to detect the cytotoxic activity of Cisplatin, Geneticin, hydromycin B and iodoacetamide, which display a slow cytotoxic effect. Cell culture conditions, cell density, compound concentration, image acquisition and analysis were the same as described above.

Evaluation of the DNS assay robustness

The Z' factor value for the DNS assay was calculated over 48 data points for 96-well plates using NIH 3T3 and YT cells prepared as described above. Z' factor assays were carried out utilizing Hydrogen peroxide (H_2O_2; Acros Organics, NJ) as a positive control for cytotoxicity at a final concentration of 300 µM (Miyoshi et al. 2006; Zierdt 1986) for 20h. Ninety-six data points for H_2O_2 treated as well as for untreated cells were used to calculate the Z' factor values in the 384-well plate format. Dye addition and image acquisition were perform as described above. The following equations were used to calculate the Z' factor value, S/N and S/B ratio values : Z' factor, $Z'=1-(3\sigma_T+3\sigma_U) / (\mu_T-\mu_U)$; signal-to-noise, $S/N= (\mu_T-\mu_U) / \sigma_U$; signal-to-background, $S/B= \mu_T / \mu_U$ (Zhang et al 1999); and the coefficient of variation percent value (%CV) for treated cells; $\%CV= (\sigma_T / \mu_T) 100$ (Inglese et al. 2007). Where σ_T is the standard deviation of the wells corresponding to the treated cells, σ_U is the standard deviation of the untreated controls, μ_T is the mean value of the wells corresponding to the treated cells, and μ_U is the mean value of the untreated controls.

Primary screening using the DNS assay

As a primary screen, experimental compounds were tested for their cytotoxicity on the NIH 3T3 cell line at a final concentration of 100 µM in the presence of 1% v/v DMSO per well and dispensed into the wells *via* a robotic pipetting system (epMotion 5070). As positive controls for cytotoxicity, cells treated with 300 µM H_2O_2 were included in each experimental plate. DMSO (Sigma), the solvent used for all chemical compounds, was added at a final concentration of 1% v/v and used for normalization purposes to account for any DMSO-induced cytotoxicity (which was negligible). Untreated cells were included in all the experiments to establish the background of dead cells provoked by cell manipulation and factors inherent to the culture system. Cells exposed to the experimental chemical compounds and the controls were incubated for a total of 20h under the conditions described above. One hour prior to image capture, the mixture of the two fluorescent dyes was dispensed into the experimental wells by the use of the onboard pipetting system of the bioimager. To discern between cytotoxic and non-cytotoxic compounds, a threshold of 2 times standard deviation (2xSD) from the mean percentage of dead cells from all the samples was applied (Malo et al. 2006) as described below.

Primary screening using the MTS assay

To establish a comparison between the DNS and MTS assays, NIH 3T3 cells were utilized at the same density as indicated above. The same 80 chemical compounds were tested at the same final concentration (100 µM) utilized with the DNS assay. After 18h of incubation, 20 µl of the MTS reagent (CellTiter 96 AQueousOne Solution Cell Proliferation Assay; Promega, Madison, WI) were added to each well and subsequently incubated for an additional 2h, completing 20h of incubation. The colored formazan product was measured by absorbance at 490 nm with a reference wavelength of 650 nm using a microplate reader ($VERSA_{max}$ microplate reader, MDS, Inc., Toronto, Canada). Control wells without cells and containing the same volumes of culture medium and MTS reagent were used as blank to subtract background absorbance. Data were expressed as percentage of cell viability relative to DMSO (solvent control) treated cells. However, in order to make the data comparable to the DNS results, the percentages of dead cells were obtained by subtracting the percentage of cell viability from 100. In this assay the same 2xSD rule (see following section) was applied to determine whether a compound was cytotoxic or not.

Cut-off value for cytotoxicity in primary screening assays

The cut-off values for the DNS and MTS primary screening assays were determined by the 2xSD rule (Malo et al 2006), where the hit threshold is defined as 2xSD beyond the mean of the screened samples. Therefore, compounds whose measured cytotoxicity were equal or exceeded the hit threshold were considered as hits. In order to determine comparable primary screening cut-off values, the 2xSD value was independently calculated for both DNS and MTS assays. Since the DNS assay was run three independent times to determine its reproducibility, the cut-off value was calculated as the mean of the individual 2xSD values derived from each experiment.

Secondary screening for hit validation

To further validate the cytotoxicity of the identified hits from the primary screening on NIH 3T3 cells, cell death was analyzed by the DNS and a flow cytometry assay. NIH 3T3 and YT cell lines were treated with a single concentration (100 µM) of chemical compound in triplicate. Cell density, culture conditions and image acquisition were performed as described above. Cell death was evaluated *via* flow cytometry using the PI staining method as previously described (Varela-Ramirez et al. 2011). YT and NIH 3T3 cells were seeded in a 96-well plate as described above and treated with test compounds for 20h. After incubation, floating NIH 3T3 cells were transferred to an ice-cold tube, while adhered cells were treated for 5 min with 0.25% of trypsin solution. Cells from each individual well, including those floating and those harvested by trypsinization, were washed with cold complete media and cold PBS, pelleted by centrifugation (1,400 rpm for 5 min at 4°C) and resuspended in 300 µl of PBS containing 10 µg/ml of PI (Shaik et al. 2009). The same protocol omitting the trypsinization step was applied for the YT cells. Cells were gently vortexed and immediately analyzed using a Cytomics FC 500 flow cytometer (Beckman Coulter, Miami, FL). For each sample, a maximum of 3,000 individual events were collected and analyzed using CXP software (Beckman Coulter, Miami, FL). All compounds were analyzed in triplicate and cytotoxicity was determined as the percentage of PI stained cells.

Generation of dose-response curves and CC_{50} values

Glass-bottomed 96-well plates were prepared and processed as described above using NIH 3T3 cells. Chemical compounds identified as hits were tested at several concentrations to create dose-response curves and determine the 50% cytotoxic concentration (CC_{50}). CC_{50} was defined as the compound concentration causing loss of membrane integrity of 50% of the cell population as compared to solvent treated cells after 20h of incubation. The CC_{50} values were obtained from linear portions of the dose-response curves as previously described (Varela-Ramirez et al 2011). Briefly, data was normalized by subtracting from each experimental value the average percentage of dead cells from six wells treated with 1% v/v DMSO (solvent control). The two compound concentrations closest to the 50% cytotoxicity value were plotted using linear regression and the CC_{50} values were extrapolated from the line equation.

RESULTS AND DISCUSSION

HTS has been amply used to screen large numbers of novel chemical compounds to identify biologically active molecules for specific targets (Baker 2010; Pereira and Williams 2007). A cell-based HTS assay should be robust, economical, sensible, reproducible and applicable to large scale plate formats (Carrol et al. 2004). The assay presented herein incorporates all of the aforementioned features of an HTS assay to rapidly and reliably determine the cytotoxic effects of a large number of compounds.

Nuclear staining is a powerful and versatile technique to detect cells and has been used broadly in biological assays (Clark 1981; Kepp et al 2011). This staining strategy is very useful to define and analyze cell populations. The differential nuclear staining assay presented here makes use of Hoechst, which is membrane permeable and detects all nucleated cells while PI only stains dead cells after membrane disruption. As shown in Figure 1C**,** the staining pattern of dead cells results in co-localized nuclear fluorescence signals (magenta color).

To accomplish optimal single-cell analysis and to obtain an appropriate number of ROIs for acquisition of statistically significant values, cell density was optimized for each cell line. Using the 2X2 montage setting and plating the NIH 3T3 and YT cells at the optimum cell densities, as indicated in MATERIAL AND METHODS, the imaging system was able to capture ~100 to 400 ROIs (cells) per well.

The validation of the assay presented here was performed using a 96-well plate format and NIH 3T3 cells for the detection of cytotoxicity after exposure to ten different compounds. The test compounds included three antibacterial agents that are non-toxic to mammalian cells (ampicillin, kanamycin and streptomycin at 100 µg/ml each) along with seven well known cytotoxic compounds. When added to NIH 3T3 cells and incubated for 20h, only titanocene (500 µM), Tween 20 (0.1% v/v) and plumbagin (20 µM) exhibited cytotoxic activity (Montoya et al. 2004; Figure 2A). As anticipated, the three antibacterial compounds did not exhibit any toxic effect. Those cytotoxic agents that did not show a cytotoxic effect at 20h were further tested at 72h and 120h along with plumbagin as a positive control for cytotoxic activity (Figure 2B). Plumbagin treatment resulted in 85.91% of dead cells at 20h and it did not change significantly after additional incubation of 72h and 120h (Figure 2B**).** At 72h of incubation, Cisplatin and Geneticin caused a significant amount in cytotoxicity, which was even more accentuated at 120h. Hygromycin B exhibited its cytotoxic activity only after 120h of incubation, whereas iodoacetamide induced cell death at 72h but its toxic effect did not increase at 120h (Figure 2B). Based on these results, the panel of toxic compounds was classified into fast- (plumbagin, titanocene and Tween 20) and slow- (Cisplatin, Geneticin hygromycin B, iodoacetamide) acting cytotoxic compounds. As expected, all of the well known toxic compounds were successfully identified as positive for cytoxicity by the DNS assay while the non-toxic compounds did not induce cell death. These experiments demonstrated that the DNS assay can be adapted

to different incubation times for detection of cytoxicity of both fast- and slow-acting compounds.

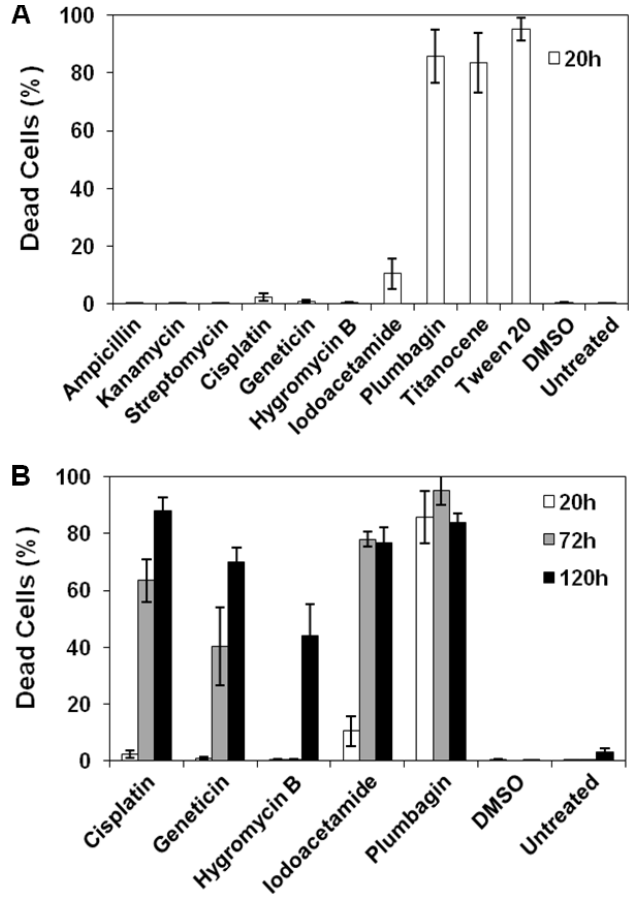

Figure 2. Assessment of cell death using the DNS assay after 20, 72, and 120 hours (h) of incubation. The concentrations of compounds that were used in this analysis were 100 µg/ml for ampicillin, kanamycin and streptomycin, 100 µM for Cisplatin, 1444 µM for Geneticin, 379 µM for hygromycin B, and 10 µM for iodoacetamide. In panel A, cells were incubated with chemical compounds for 20h to detect fast-acting toxic activity. In panel B, three incubation times were performed at 20, 72 and 120h to identify slow-acting toxic compounds. In addition, 20 µM of plumbagin was utilized as a positive control of cytotoxicity. DMSO, which was used to dissolve Plumbagin, was tested at a final concentration of 1% v/v as a solvent control. Untreated cells were used as an indicator of cellular viability during all the incubation time periods. NIH 3T3 cell seeding and images capture procedures are described in detail in the MATERIAL and METHODS section. Each bar represents the average value of three independent measurements, and error bars represent standard deviation of the mean.

The Z' factor, a well-known parameter for quality assessment in assay development and optimization (Zhang et al 1999), has been widely utilized to validate cell-based assays suitability for HTS (An and Tolliday 2010). It assesses the screening data variability, by taking into account the mean and standard deviation of positive and negative controls, to determine whether an assay can identify hits with confidence. A Z' factor between 0 and 0.5 reflects too much overlap among the positive and negative controls and denotes an assay not suitable for HTS, whereas a Z' factor in the range of 0.5 to 1 indicates an assay highly suitable for HTS. In order to determine if the DNS assay is applicable for HTS, the Z' factor was calculated using NIH 3T3 and YT cells treated with H_2O_2. As expected, treatment with high concentrations H_20_2 inflicted a strong cytotoxic effect on both cell lines (Figure 3). To further validate the utility of the DNS assay for HTS, it was scaled-up to the 384-well format. As can be seen in Figure 3, the Z' factor values obtained for 96-well plates ranged from 0.78 to 0.86 (Figure 3A and B), while that for the 384-well format, ranged from 0.60 to 0.76 (Figure 3C and D), indicating that the DNS assay is suitable for high content screening in both plate formats. The still acceptable but slightly lower Z' factor values for the 384-well format, could be due to multiple factors such as surface-to-volume ratio, gas exchange, evaporation effects, and differences in the culture plates themselves (Gaines Das and Meager 1995). The use of adherent and non-adherent cell lines allowed us to determine if there was a major difference in the Z' factor's between the two distinct cell types. As shown in Figure 3, the Z' factor values obtained with both cell lines ranged from 0.60 to 0.86. Although the Z' factor is a very well established quality parameter for a HTS assay, it is not the only factor that should be considered. Therfore, three other parameters were also analyzed. The S/N ratio values obtained for 96-well plates ranged from 15 to 60 (Figure 3A and B), while that for the 384-well plate format ranged from 50 to 228; an acceptable S/N value should be >10. Likewise, the S/B ratio values ranged from 65 to 69 for the 96-well plate format and 46 to 305 for the 384-well plate format (Figure 3C and D); an acceptable S/B value should be >2 (Inglese et al. 2007). These analyses reveled that the DNS assay is suitable for high content screening in both multiwell plate formats. These results denote high reproducibility of the assay. In addition, intra-plate, inter-plate and day-to-day variability should yield %CV <15% (Inglese et al. 2007). The %CV values for treated cells in 96-well and 384-well plate formats were ≤ 11.74%; thus demonstrating excellent reproducibility (Figure 3). Based on all the values obtained for the multiple assay parameters commonly used for quality assessment of HTS assays, the DNS assay was found to be highly suitable for HTS initiatives.

Moreover, to obtain more informative data related to the reproducibility of this assay, three independent experiments analyzing the 80 experimental compounds were prepared as already described, on different days and utilizing different batches of NIH 3T3 cells. Assay performance was monitored to ensure plate-to-plate reproducibility. The three multiwell plates were processed similarly as described above. Figure 4 shows the mean and standard deviation from three replicas of

each compound. The standard deviation values of 74 experimental compounds were of 5 or less, five compounds yielded values between 5 and 10, and only one compound yielded a standard deviation greater than 10 (11.2).

As proof of concept, the 80 experimental chemical compounds from a small molecule library were screened on a 96-well plate format using adherent NIH 3T3 cells in the presence of the compounds at a final concentration of 100 µM after 20h. From this analysis, six compounds were identified as hits with cytotoxic values equal or higher than the cut-off value of 51.37% (Figure 4A; see section in MATERIAL AND METHODS). The molecular structures and names of the compounds identified as hits are annotated in Figure 5. As controls, untreated and solvent treated (DMSO) cells were used along with H_2O_2 as a positive cytotoxic control in all assays. In addition, the MTS assay, which has been extensively applied to assess viability, was used for comparison purposes using the same 80 compounds evaluated by the DNS assay. The MTS assay was utilized since the Z' factor (0.70) for this assay was previously found to be adequate for HTS projects (Yip et al. 2006). In an effort to make the DNS and MTS assays comparable, the threshold for each assay was set at two standard deviations (2xSD) from the respective mean value and the same cell culture and compound exposure conditions were used. As can be seen in Figure 4B, the MTS assay also detected the six compounds that were previously identified by DNS. This result suggests that DNS's effectiveness to identify cytotoxic compounds is comparable to the commonly used MTS assay. Although the assays would appear comparable, the MTS assay gives high background that can be interpreted as a hit depending on the thresholds utilized (see Figure 4B for example). MTS-based assays are being amply used to monitor cellular viability when in essence this assay measures metabolic activity (Kepp et al. 2011).

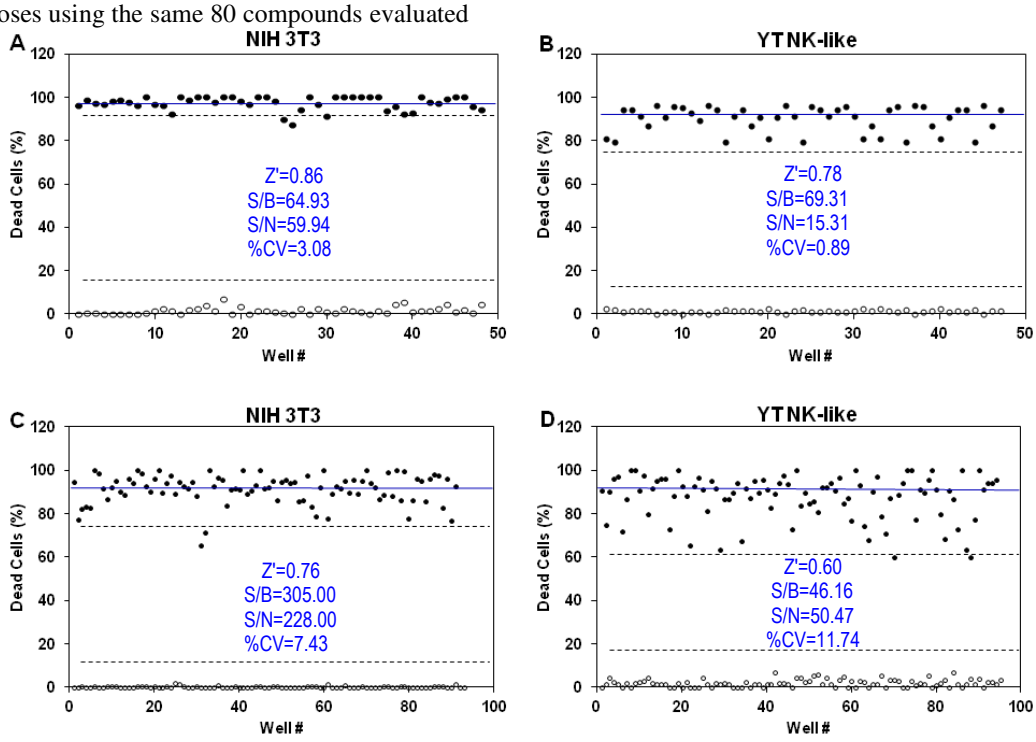

Figure 3. Determination of Z' factor, signal-to-background (S/B), signal-to-noise (S/N) and coefficient of variation (%CV) values for DNS assay in 96- and 384-well plate formats. The Z' factor was calculated individually for NIH 3T3 (panels A and C) and YT (panels B and D) cells, in 96-well (panels A and B) and 384-well (panels C and D) multiwell plate formats. Untreated cells (negative controls) and cells exposed to 300 µM H_20_2 (positive controls) were compared in series of 48 and 96 replicates, for 96- and 384-well plates, respectively. Each plot show the scatter distribution of positive (black circles, located at the top) and negative (open circles, located at the bottom) controls for cytotoxicity. Also in each plot, the mean of the positive controls (solid horizontal blue line, close to top) and their 3xSD values (large dashed horizontal line), as well as the 3xSD values of the negative controls (small dashed horizontal line, close to the *x* axis) are indicated. The mean of the negative controls overlapped with the *x* axis in most cases, and it was omitted. The label in the *y* axis indicates the percentage of dead cells, while that in the *x* axis indicates the well number. Z' factor values are annotated in the middle of the plot (in blue), they ranged from 0.78 to 0.86 for the 96-well plate, whereas for 384-well plates were from 0.60 to 0.76. Additionally, S/B and S/N ratios, as well as %CV of the positive controls are also annotated. Suitable values for Z' factor, S/N, S/B and %CV are >0.5, >10, >2 and <15%, respectively.

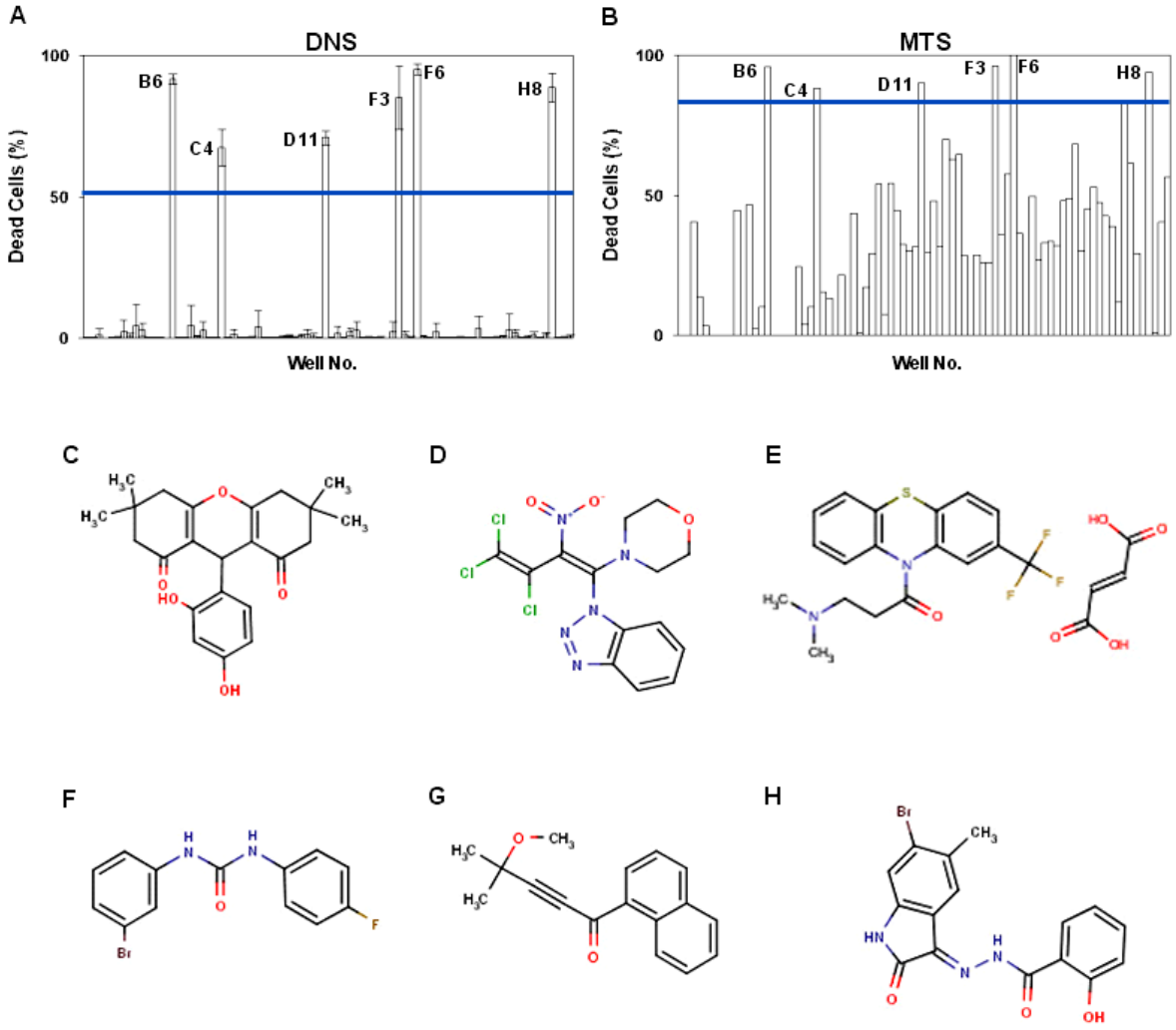

Figure 4. Hit identification by primary screening of experimental compounds using DNS (panel A) and MTS (panel B) assays. Each of the 80 experimental compounds was tested on NIH 3T3 cells at a 100 µM final concentration, for both assays, using a 96-well plate format. In panel A**,** each bar indicates the average value and its standard deviation of three independent experiments. The cytotoxicity thresholds (2xSD) for each assay are indicated in the graphs by a solid horizontal blue line, situated at 51.37% for DNS and 85.29% for the MTS assay. In panel A, the threshold represents the average of the 2xSD threshold values obtained from each of the three independent experiments. Chemical compounds identified as hits, with cytotoxicity equal or above the threshold value are annotated in the graphs. Compounds are named by their position inscribed in the experimental 96-well plate: B6, C4, D11, F3, F6 and H8. The *y* axis represents the percentage of dead cells, while well number is indicated on the *x* axis. In panels C to H, the six chemical compound structures identified as hits using DNS and MTS assays. Compounds C, D, E and G, were soluble in cell culture medium at a concentration of 100 µM, whereas compound F and H formed crystals under the same conditions. Due to their solubility**,** compounds C, D, E and G were further validated in a secondary screening *via* DNS and flow cytometry methods. The well number as inscribed in the 96-well plate (the capital letter correspond to the row and the number to the column), the ChemBridge ID number and name of experimental chemical compound are as follow: panel C**,** B6, 5213683, 9-(2,4-dihydroxyphenyl)-3,3,6,6-tetramethyl-3,4,5,6,7,9-hexahydro-1H-xanthene-1,8(2H)-dione**;** panel D, C4, 5213373, 1-[3,4,4-trichloro-1-(4-morpholinyl)-2-nitro-1,3-butadien-1-yl]-1H-1,2,3-benzotriazole; panel E, D11, 5216189, N,N-dimethyl-3-oxo-3-[2-(trifluoromethyl)-10H-phenothiazin-10-yl]-1-propanamine 2-butenedioate; panel F**,** F3, 5214382, N-(3-bromophenyl)-N'-(4-fluorophenyl)urea; panel G, F6, 5213809, 4-methoxy-4-methyl-1-(1-naphthyl)-2-pentyn-1-one; and panel H, H8, 5214873, N'-(6-bromo-5-methyl-2-oxo-1,2-dihydro-3H-indol-3-ylidene)-2-hydroxybenzohydrazide.

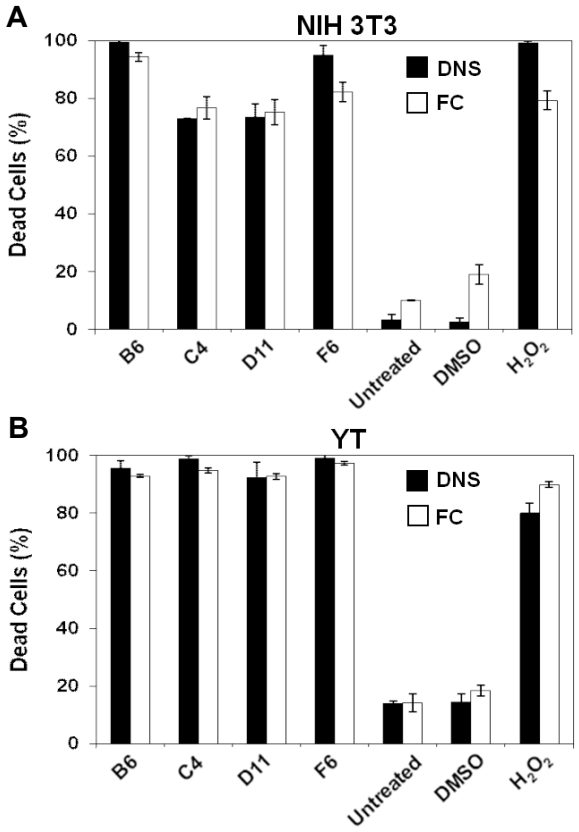

Figure 5. Secondary screening for hit validation utilizing DNS and flow cytometry assays. Four out of the six hit compounds identified by the primary screening were further analyzed on NIH 3T3 (panel A) and YT (panel B) cells in triplicate by DNS (filled black bars) and flow cytometry (FC; open bars) under the same experimental conditions. Two compounds (F3 and H8) identified as hits were excluded from these analyses since they came out of solution and formed crystals that interfered with flow cytometry. Untreated cells, solvent-treated cells (1% v/v DMSO), and H_2O_2 (300 µM) treated cells were added as controls. Each bar represents the mean value of three measurements and error bars correspond to the standard deviation of the mean. Compounds are annotated by their position inscribed in the experimental 96-well plate: B6, C4, D11, and F6. In panel A, the standard deviation obtained with DNS assay for C4 (filled black bar) is not very evident since the value was very small (0.1).

Our results have revealed that the DNS assay is more reliable in measuring viability as it measures PI-positive nuclei of dead cells while the MTS assay cannot distinguish between cytotoxic effects and metabolic inactivity (Kepp et al. 2011). In particular, we have noticed that cells that were clearly damaged by microscopic inspection and exhibited signs of cell death (membrane blebbing and nuclear condensation) by compound treatment can on occasion give readouts indicative of undamaged living cells (our unpublished observations).

To validate the results from the primary screen, a secondary screen of the identified hit compounds was conducted on the NIH 3T3 and YT cell lines by the DNS and flow cytometry assays (Figure 5). Two of the six compounds identified in the primary screen were eliminated from the secondary screen since these were found to precipitate out of solution and their final concentration could not be determined. Nevertheless, the presence of crystals did not affect the detection of cytotoxic compounds when using the DNS or MTS assays. In contrast, when using flow cytometry, the cytotoxic values were significantly altered because compound crystals were counted as live cells (data not shown). The four remaining soluble compounds (B6, 5213683, 9-(2,4-dihydroxyphenyl)-3,3,6,6-tetramethyl-3,4,5,6,7,9-hexahydro-1H-xanthene-1,8(2H)-dione; C4, 1-[3,4,4-trichloro-1-(4-morpholinyl)-2-nitro-1,3-butadien-1-yl]-1H-1,2,3-benzotriazole; D11, N,N-dimethyl-3-oxo-3-[2-(trifluoromethyl)-10H-phenothiazin-10-yl]-1-propanamine 2-butenedioate; F6, 4-methoxy-4-methyl-1-(1-naphthyl)-2-pentyn-1-one) were re-evaluated in triplicate under the same experimental conditions applied during the primary screen. As expected, the four hits were found to be highly cytotoxic in both DNS and flow cytometry assays (Figure 5); thus validating the primary screening results. This high rate of hit validation (100%) demonstrates the suitability and reproducibility of the DNS assay. In fact, the four compounds showed similar cytotoxic effects on both cell lines by both assays (Figure 5).

Additionally, to evaluate the effectiveness of the DNS assay for secondary screening, dose-response curves and the CC_{50} values were determined (Figure 6). As anticipated, cytotoxicity was significantly increased with a concomitant increase in compound concentration. Using a wide range of compound concentrations, the CC_{50} was calculated (see MATERIAL AND METHODS and Varela-Ramirez et al 2011). As positive controls for cytotoxicity, several concentrations of H_2O_2 were utilized to generate a dose response curve and determine the CC_{50} value (23.23 µM; see Figure 6E and F). The CC_{50} values determined for the four tested compounds were in descending order: 33.05 µM for D11, 25 µM for B6, 3.23 µM for C4, and 0.99 µM for F6; the latter being the most toxic (Figure 6). Figure 7 shows representative images of cells treated with several concentrations of B6 that were used to generate the dose-response curves.

Summary

The Hoechst/PI DNS assay offers several advantages which are summarized below:

1. The assay does not require removal of media, any washes or centrifugation steps. The dye mixture is inexpensive, easy to prepare, stable at room temperature and compatible with robotic pipetting systems. In addition, staining takes place during the last hour of the incubation period, which provides convenience and flexibility in capturing the images and minimizes dye exposure time.

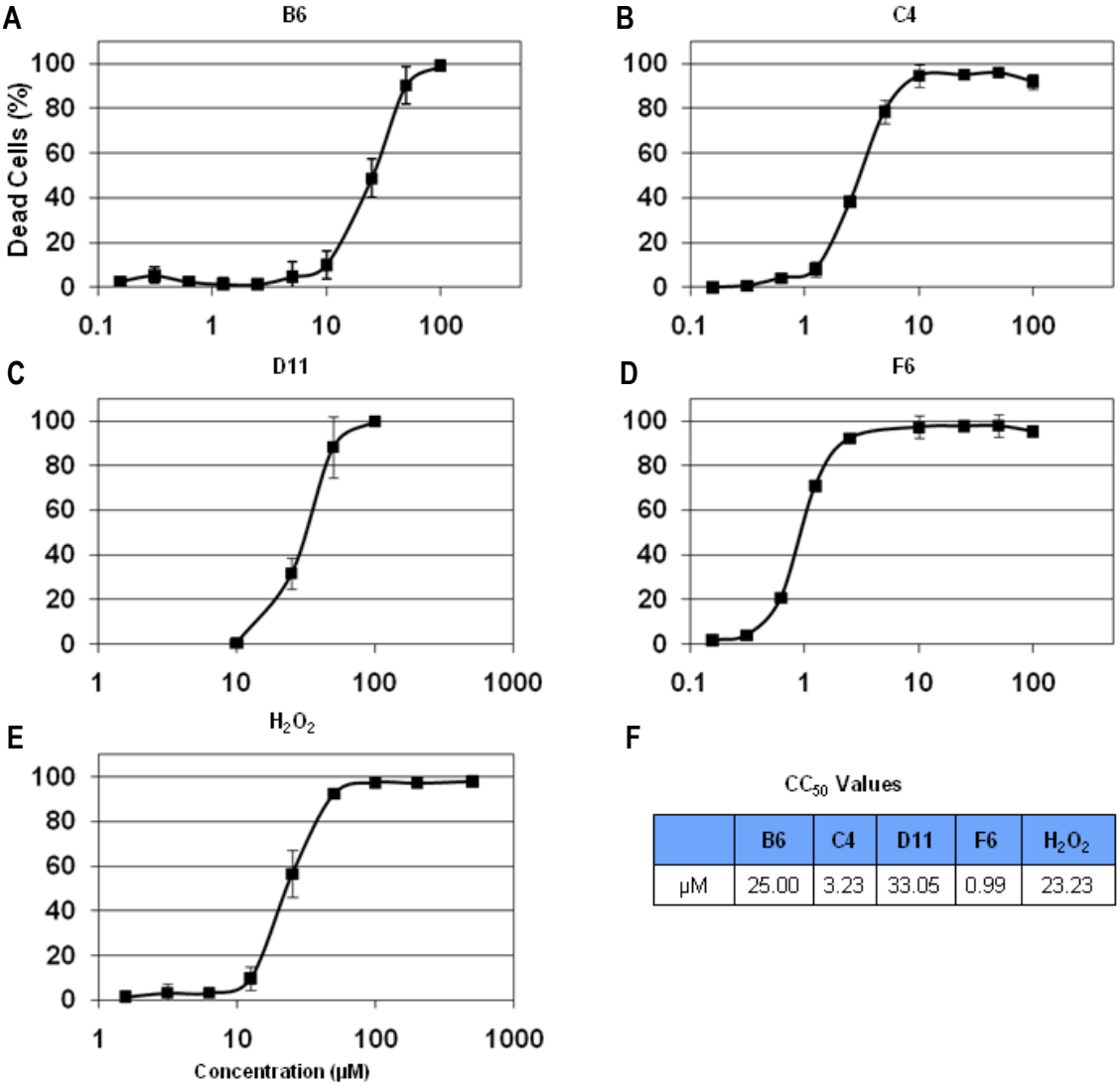

	B6	C4	D11	F6	H_2O_2
µM	25.00	3.23	33.05	0.99	23.23

Figure 6. Dose-response curves and determination of CC_{50} values utilizing the DNS assay. Dose-response effect and CC_{50} were determined on NIH 3T3 cells for the identified and validated hits. For this analysis, cells were exposed for 20h to increasing concentrations of experimental compounds; B6 (panel A); C4 (panel B); D11 (panel C); F6 (panel D); and H_2O_2 (panel E). In each graph, the percentage of dead cells is shown on the *y* axis while the compounds concentrations (µM) are shown in the *x* axis. Each data point in the graphs represents the mean percentage of dead cells at each dose and the error bars correspond to the standard deviation from series of six replicates. In panel F, the CC_{50} values (µM) for four experimental compounds and H_2O_2 on NIH 3T3 cells were derived as described in MATERIAL AND METHODS. Compounds are annotated by their position in the original 96-well microplate purchased from ChemBridge Co. (San Diego, CA).

2. In contrast to flow cytometry, cell imaging analysis is not impaired by artifacts such as cell debris or insoluble complexes; thus providing a high degree of objectivity and sensitivity.

3. The effect of a specific compound can be re-evaluated by visual inspection of captured images. The output is quantitative since the actual number of dead cells is automatically calculated with respect to total cell number and different thresholds can be applied to increase or decrease the stringency of detection.

4. The assay is robust and applicable to high content primary screens for identification of hits with cytotoxic activity. In addition, the assay can be used for secondary screening to validate hits and to generate dose-response curves and CC_{50} values.

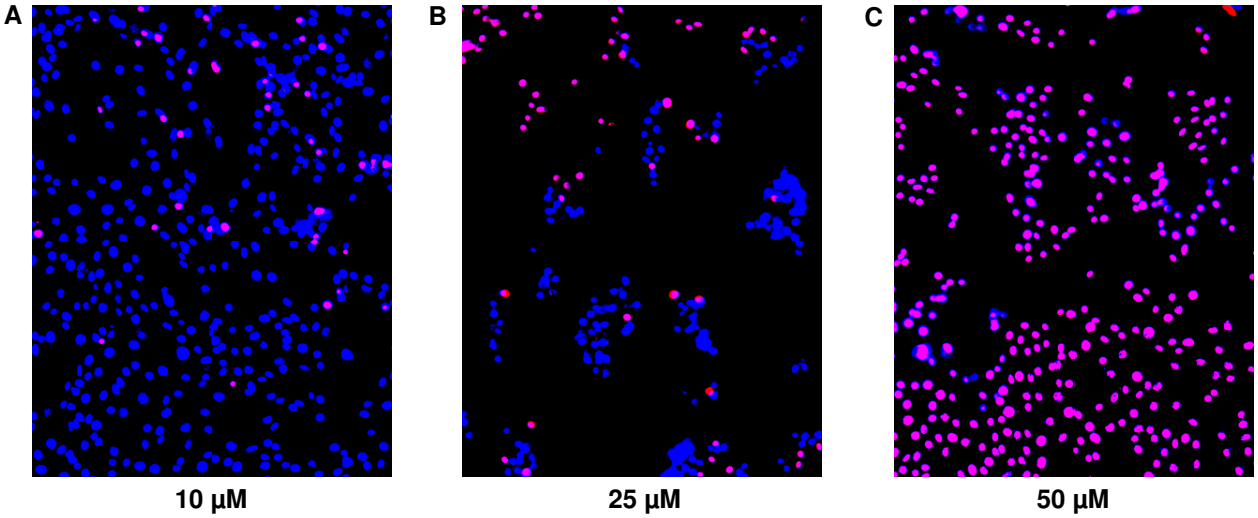

Figure 7. Representative overlay 2X2 montage images of cells treated at increasing compound concentrations. NIH 3T3 cells were utilized as described in MATERIAL AND METHODS and exposed for 20h to concentrations of 10 µM (panel A), 25 µM (panel B) and 50 µM (panel C) of B6 (9-(2,4-dihydroxyphenyl)-3,3,6,6-tetramethyl-3,4,5,6,7,9-hexahydro-1H-xanthene-1,8(2H)-dione). Cells with intact and damaged plasma membrane were stained with Hoechst and their nuclei are shown in blue. Cells with compromised plasma membrane resulted in double staining with Hoechst and PI, which are shown in magenta as a consequence of colocalized signals of the two fluorescence channels.

5. The assay is compatible with single end-point screens as well as with time-course settings where multiple readouts are generated from the same well at different time-points.

ACKNOWLEDGMENTS

The authors would like to express special thanks to Dr. Robert Kirken at the Department of Biological Sciences of The University of Texas at El Paso for the generous gift of the YT cell line, Dr. Ting Qian at BD Biosciences for valuable recommendations on the usage of the bioimager system and Dr. Julia Bader at the Statistical Consulting Laboratory of The University of Texas at El Paso for advice on the statistical measures that were conducted. This work was performed within the Cell Culture and High Throughput Screening Core Facility, Biomolecule Analysis Core Facility, and DNA Analysis Core Facility of The University of Texas at El Paso supported by RCMI Grant No. 5G12RR008124 to the Border Biomedical Research Center (BBRC) from the National Center for Research Resources (NCRR), a component of the NIH.

Abbreviations: ATCC, American Type Culture Collection; B6, 9-(2,4-dihydroxyphenyl)-3,3,6,6-tetramethyl-3,4,5,6,7,9-hexahydro-1H-xanthene-1,8(2H)-dione; C4, 1-[3,4,4-trichloro-1-(4-morpholinyl)-2-nitro-1,3-butadien-1-yl]-1H-1,2,3-benzotriazole; CC_{50}, Concentration that results in 50% cytotoxicity; %CV, percent coefficient of variation; D11, N,N-dimethyl-3-oxo-3-[2-(trifluoromethyl)-10H-phenothiazin-10-yl]-1-propanamine 2-butenedioate; DMEM, Dulbecco's modified Eagle medium; DMSO, Dimethyl sulfoxide; DNS, Differential nuclear staining; F6, 4-methoxy-4-methyl-1-(1-naphthyl)-2-pentyn-1-one; GFP, Green fluorescence protein; H8, N'-(6-bromo-5-methyl-2-oxo-1,2-dihydro-3H-indol-3-ylidene)-2-hydroxybenzohydrazide; H_2O_2, Hydrogen peroxide; Hoechst, Hoechst 33342; HTS, High-throughput screening; LDH, Lactate dehydrogenase; MTT, 3-(4,5-dimethylthiazol-2-yl)-2,5-diphenyltetrazolium bromide); MTS, 3-(4,5-dimethylthiazol-2-yl)-5-(3-carboxymethoxyphenyl)-2-(4-sulfophenyl)-2H-tetrazolium); NK, Natural killer; PBS, Phosphate buffered saline; PI, Propidium iodide; ROIs, Regions of interest; RPMI, Roswell Park Memorial Institute; S/B, Signal-to-background ratio; S/N, Signal-to-noise ratio; 2xSD, Two times standard deviation; 3xSD, Three times standard deviation; µM, Micromolar; YT, YT NK-like.

REFERENCES

Aguilera RJ, Montoya J, Primm TP, Varela-Ramirez A, 2006. Green fluorescent protein as a biosensor for toxic compounds. Reviews in fluorescence 3: 463-476

Ahmed AA, Lu Z, Jennings NB, Etemadmoghadam D, Capalbo L, Jacamo RO, et al, 2010. SIK2 is a centrosome kinase required for bipolar mitotic spindle formation that provides a potential target for therapy in ovarian cancer. Cancer Cell 18: 109-12

An WF, Tolliday N, 2010. Cell-Based Assays for High-Throughput Screening. Mol Biotechnol 45: 180-186

Baker M, 2010. Academic screening goes high-throughput. Nature Methods 7:787-792

Bartholomeusz GA, Talpaz M, Kapuria V, Kong LY, Wang S, Estrov Z, et al, 2007. Activation of a novel Bcr/Abl destruction pathway by WP1130 induces apoptosis of chronic myelogenous leukemia cells. Blood 109: 3470-3478

Batchelor RH, Zhou M, 2004. Use of cellular glucose-6-phosphate dehydrogenase for cell quantitation: applications in cytotoxicity and apoptosis assays. Anal Biochem 329: 35-42

Boyum A, 1968. Isolation of mononuclear cells and granulocytes from human blood. Isolation of monuclear cells by one centrifugation, and of granulocytes by combining centrifugation and sedimentation at 1 g. Scand J Clin Lab Invest Suppl 97: 77-89

Breier JM, Radio NM, Mundy WR, Shafer TJ, 2008. Development of a high-throughput screening assay for chemical effects on proliferation and viability of immortalized human neural progenitor cells. Toxicol Sci 105: 119-133

Bruggisser R, von Daeniken K, Jundt G, Schaffner W, Tullberg-Reinert H, 2002. Interference of plant extracts, phytoestrogens and antioxidants with the MTT tetrazolium assay. Planta Med 68: 445-448

Carrol SS, Inglese J, Mao SS, Olsen DB, 2004.Drug screening: Assay development issues. In: Prendegast, GC (ed.) Molecular Cancer Therapeutics: Strategies for drug discovery and development, John Wiley & Sons, Inc.

Chan GK, Richards GR, Peters M, Simpson PB, 2005. High content kinetic assays of neuronal signaling implemented on BD pathway HT. Assay Drug Dev Technol 3: 623-636

Ciancio G, Pollak A, Taupier MA, Block NL, Irvin GLr, 1988. Measurement of cell-cycle phase-specific cell death using Hoechst 33342 and propidium iodide: preservation by ethanol fixation. J Histochem Cytochem 36: 1147-1152

Clark G. 1981. Staining procedures. Williams and Wilkins, Baltimore, MD, USA

Cordeiro MF, Guo L, Coxon KM, Duggan J, Nizari S, Normando EM, et al, 2010. Imaging multiple phases of neurodegeneration: a novel approach to assessing cell death in vivo. Cell Death and Disease 1:1-10.

Decker T, Lohmann-Matthes ML, 1988. A quick and simple method for the quantitation of lactate dehydrogenase release in measurements of cellular cytotoxicity and tumor necrosis factor (TNF) activity. J Immunol Methods 115: 61-69

Dive C, Gregory CD, Phipps DJ, Evans DL, Milner AE, Wyllie AH, 1992. Analysis and discrimination of necrosis and apoptosis (programmed cell death) by multiparameter flow cytometry. Biochim Biophys Acta 1133:275-285

Dragunow M, 2008. High-content analysis in neuroscience. Nat Rev Neurosci 9: 779-788

Engel JC, Ang KK, Chen S, Arkin MR, McKerrow JH, Doyle PS, 2010. Image-based high-throughput drug screening targeting the intracellular stage of Trypanosoma cruzi, the agent of Chagas' disease. Antimicrob Agents Chemother 54: 3326-3334

Gaines Das RE, Meager A, 1995. Evaluation of assay designs for assays using microtitre plates: results of a study of in vitro bioassays and immunoassays for tumour necrosis factor (TNF). Biologicals 23: 285-297

Gonzalez-Nicolini V, Fussenegger M, 2005. In vitro assays for anticancer drug discovery--a novel approach based on engineered mammalian cell lines. Anticancer Drugs 16: 223-228

Goto H, Yang B, Petersen D, Pepper KA, Alfaro PA, Kohn DB, et al, 2003. Transduction of green fluorescent protein increased oxidative stress and enhanced sensitivity to cytotoxic drugs in neuroblastoma cell lines. Mol Cancer Ther 2: 911-917

Inglese J, Johnson RL, Simeonov A, Xia M, Zheng W, Austin CP, et al, 2007. High-throughput screening assays for the identification of chemical probes. Nat Chem Biol 3: 466-479

Kepp O, Galluzzi L, Lipinski M, Yuan J, Kroemer G, 2011. Cell death assays for drug discovery. Nat Rev Drug Discov 10: 221-237.

Kim YE, Chen J, Chan JR, Langen R, 2009. Engineering a polarity-sensitive biosensor for time-lapse imaging of apoptotic processes and degeneration. Nat Methods 7: 67-73

Kroemer G, El-Deiry WS, Golstein P, Peter ME, Vaux D, Vandenabeele P, et al, 2005. Classification of cell death: recommendations of the Nomenclature Committee on Cell Death. Cell Death Differ 12 Suppl 2: 1463-1467

Lau AC, Cui H, Tymianski M, 2007. The use of propidium iodide to assess excitotoxic neuronal death in primary mixed cortical cultures. Methods Mol Biol 399: 15-29

Malo N, Hanley JA, Cerquozzi S, Pelletier J, Nadon R, 2006. Statistical practice in high-throughput screening data analysis. Nat Biotechnol 24: 167-175

Miyawaki A, Nagai T, Mizuno H, 2005. Engineering fluorescent proteins. Adv Biochem Eng Biotechnol 95: 1-15

Miyoshi N, Oubrahim H, Chock PB, Stadtman ER, 2006. Age-dependent cell death and the role of ATP in hydrogen peroxide-induced apoptosis and necrosis. Proc Natl Acad Sci U S A 103: 1727-1731

Montoya J, Varela-Ramirez A, Estrada A, Martinez LE, Garza K, Aguilera RJ, 2004. A fluorescence-based rapid screening assay for cytotoxic compounds. Biochem Biophys Res Commun 325: 1517-1523

Montoya J, Varela-Ramirez A, Shanmugasundram M, Martinez LE, Primm TP, Aguilera RJ, 2005. Tandem screening of toxic compounds on GFP-labeled bacteria and cancer cells in microtiter plates. Biochem Biophys Res Commun 335: 367-372

Nohara LL, Lema C, Bader JO, Aguilera RJ, Almeida IC, 2010. High-content imaging for automated determination of host-cell infection rate by the intracellular parasite Trypanosoma cruzi. Parasitol Int 59: 565-570

Parks DR, Bryan VM, Oi VT, Herzenberg LA, 1979. Antigen-specific identification and cloning of hybridomas with a fluorescence-activated cell sorter. Proc Natl Acad Sci U S A 76: 1962-1966

Pepperkok R, Ellenberg J, 2006. High-throughput fluorescence microscopy for systems biology. Nat Rev Mol Cell Biol 7: 690-696

Pereira DA, Williams JA, 2007. Origin and evolution of high throughput screening. Br J Pharmacol 152: 53-61

Riss T, Moravec R, 2002. Introducing the CytoTox-ONE homogeneous membrane integrity assay. CellNotes 4: 6-9

Romanha AJ, Castro SL, Soeiro Mde N, Lannes-Vieira J, Ribeiro I, Talvani A, et al, 2010. In vitro and in vivo experimental models for drug screening and development for Chagas disease. Mem Inst Oswaldo Cruz 105: 233-238

Rosado A, Zanella F, Garcia B, Carnero A, Link W, 2008. A dual-color fluorescence-based platform to identify selective inhibitors of Akt signaling. PLoS One 3: e1823

Sasaki T, Ohno T, 1994. Cytotoxicity tests on eye drop preparations by LDH release assay in human cultured cell lines. Toxicol In Vitro 8: 1113-1119

Shaik N, Martinez A, Augustin I, Giovinazzo H, Varela-Ramirez A, Sanau M, et al, 2009. Synthesis of apoptosis-inducing iminophosphorane organogold(III) complexes and study of their interactions with biomolecular targets. Inorg Chem 48: 1577-1587

Siqueira-Neto JL, Song OR, Oh H, Sohn JH, Yang G, Nam J, et al, 2010. Antileishmanial high-throughput drug screening reveals drug candidates with new scaffolds. PLoS Negl Trop Dis 4: e675

Stohr M, Vogt-Schaden M, 1980. A new dual staining technique for simultaneous flow cytometric DNA analysis of living and dead cells. In: Laerum, OD, Lindmo, T, Thorud, E (eds.) Flow Cytometry Vol. IV, Universitetsforlaget, Bergen, Norway, pp 96-99

Szafran AT, Szwarc M, Marcelli M, Mancini MA, 2008. Androgen receptor functional analyses by high throughput imaging: determination of ligand, cell cycle, and mutation-specific effects. PLoS One 3: e3605

Tian H, Ip L, Luo H, Chang DC, Luo KQ, 2007. A high throughput drug screen based on fluorescence resonance energy transfer (FRET) for anticancer activity of compounds from herbal medicine. Br J Pharmacol 150: 321-334

Varela-Ramirez A, Costanzo M, Carrasco YP, Pannell KH, Aguilera RJ, 2011. Cytotoxic effects of two organotin compounds and their mode of inflicting cell death on four mammalian cancer cells. Cell Biol Toxicol 27: 159-168

Verkhusha VV, Lukyanov KA, 2004. The molecular properties and applications of Anthozoa fluorescent proteins and chromoproteins. Nat Biotech 22: 289-296

Wallen CA, Higashikubo R, Roti Roti JL, 1983. Comparison of the cell kill measured by the Hoechst-propidium iodide flow cytometric assay and the colony formation assay. Cell Tissue Kinet 16: 357-365

Wang P, Henning SM, Heber D, 2010. Limitations of MTT and MTS-based assays for measurement of antiproliferative activity of green tea polyphenols. PLoS One 5: e10202

Yip KW, Mao X, Au PY, Hedley DW, Chow S, Dalili S, et al, 2006. Benzethonium chloride: a novel anticancer agent identified by using a cell-based small-molecule screen. Clin Cancer Res 12: 5557-5569

Yodoi J, Teshigawara K, Nikaido T, Fukui K, Noma T, Honjo T, et al, 1985. TCGF (IL 2)-receptor inducing factor(s). I. Regulation of IL 2 receptor on a natural killer-like cell line (YT cells). J Immunol 134: 1623-1630

Yuhas JM, Toya RE, Pazmino NH, 1974. Neuraminidase and cell viability: failure to detect cytotoxic effects with dye-exclusion techniques. J Natl Cancer Inst 53: 465-468

Zanella F, Rosado A, Garcia B, Carnero A, Link W, 2008. Chemical genetic analysis of FOXO nuclear-cytoplasmic shuttling by using image-based cell screening. Chembiochem 9: 2229-2237

Zhang J, Campbell RE, Ting AY, Tsien RY, 2002. Creating new fluorescent probes for cell biology. Nat Rev Mol Cell Biol 3: 906-918

Zhang JH, Chung TD, Oldenburg KR, 1999. A simple statistical parameter for use in evaluation and validation of high throughput screening assays. J Biomol Screen 4: 67-73

Zierdt CH, 1986. Simplified lysed-blood culture technique. J Clin Microbiol 23: 452-455